Effects of vertex truncation of polyhedral nanostructures on localized surface plasmon resonance

W. Y. Ma[1], J. Yao[1*], H. Yang[1], J. Y. Liu[1], F. Li[1], J. P. Hilton[2] and Q. Lin[2]

[1]*State Key Lab of Optical Technologies for Microfabrication, Institute of Optics and Electronics, Chinese Academy of Science, Chengdu, 610209, People's Republic of China*

[2]*Department of Mechanical Engineering, Columbia University, New York, NY 10027, U.S.A.*

**junyao@ioe.ac.cn*

Abstract: Polyhedral nanostructures are widely used to enable localized surface plasmon resonance (LSPR). In practice, vertices of such structures are almost always truncated due to limitations of nanofabrication processes. This paper studies the effects of vertex truncation of polyhedral nanostructures on the characteristics of LSPR sensing. The optical properties and sensing performance of triangular nanoplates with truncated vertices are investigated using electrodynamics analysis and verified by experiment. The experimental results correlated with simulation analysis demonstrate that the fabricated triangular nanoplate array has a truncation ratio, defined as the length of truncation along an edge of the triangle over the edge length, of approximately 12.8%. This significantly influences optical properties of the nanostructures, resulting in poorer sensing performance. These insights can be used to guide the design and fabrication of nanostructures for high performance LSPR sensors.

OCIS codes: (240.6680) surface plasmons; (260.3910) Metal optics; (280.4788) Optical sensing and sensors

References and Links

1. J. N. Anker, W. P. Hall, O. Lyandres, N. C. Shah, J. Zhao, and R. P. Van Duyne, "Biosensing with plasmonic nanosensors," Nat. Mater. **7**(6), 442–453 (2008).
2. M. Li, Z. S. Zhang, X. Zhang, K. Y. Li, and X. F. Yu, "Optical properties of Au/Ag core/shell nanoshuttles," Opt. Express **16**(18), 14288–14293 (2008).
3. F. Hao, C. L. Nehl, J. H. Hafner, and P. Nordlander, "Plasmon resonances of a gold nanostar," Nano Lett. **7**(3), 729–732 (2007).

#113653 - $15.00 USD Received 1 Jul 2009; revised 24 Jul 2009; accepted 25 Jul 2009; published 10 Aug 2009

4. K. L. Kelly, E. Coronado, L. L. Zhao, and G. C. Schatz, "The optical properties of metal nanoparticles: the Influence of size, shape, and dielectric environment," J. Phys. Chem. B **107**(3), 668–677 (2003).
5. M. M. Miller, and A. A. Lazarides, "Sensitivity of metal nanoparticle surface plasmon resonance to the dielectric environment," J. Phys. Chem. B **109**(46), 21556–21565 (2005).
6. P. K. Jain, I. H. El-sayed, and M. A. El-sayed, "Au nanoparticles target cancer," Nano Today **2**(1), 18–29 (2007).
7. S. L. Zhu, F. Li, C. L. Du, and Y. Q. Fu, "A localized surface plasmon resonance nanosensor based on rhombic Ag nanoparticle array," Sens. Actuators B Chem. **134**(1), 193–198 (2008).
8. K. A. Willets, and R. P. V. Duyne, "Localized surface plasmon spectroscopy and sensing," Annu. Rev. Chem. **58**(1), 267–297 (2007).
9. C. D. Chen, S. F. Cheng, L. K. Chau, and C. R. C. Wang, "Sensing capability of the localized surface plasmon resonance of gold nanorods," Biosens. Bioelectron. **22**(6), 926–932 (2007).
10. J. Becker, I. Zins, A. Jakab, Y. Khalavka, O. Schubert, and C. Sönnichsen, "Plasmonic focusing reduces ensemble linewidth of silver-coated gold nanorods," Nano Lett. **8**(6), 1719–1723 (2008).
11. J. M. McLellan, A. Siekkinen, J. Chen, and Y. Xia, "Comparison of the surface-enhanced Raman scattering on sharp and truncated silver nanocubes," Chem. Phys. Lett. **427**(1-3), 122–126 (2006).
12. S. L. Zhu, C. L. Du, and Y. Q. Fu, "Fabrication and characterization of rhombic silver nanoparticles for biosensing," Opt. Mater. **31**(6), 769–774 (2009).
13. G. H. Chan, J. Zhao, G. C. Schatz, and R. P. V. Duyne, "Localized Surface Plasmon Resonance Spectroscopy of Triangular Aluminum Nanoparticles," J. Phys. Chem. C **112**(36), 13958–13963 (2008).
14. B. J. Wiley, Y. Chen, J. M. McLellan, Y. Xiong, Z. Y. Li, D. Ginger, and Y. Xia, "Synthesis and optical properties of silver nanobars and nanorice," Nano Lett. **7**(4), 1032–1036 (2007).
15. Y. Xia, N. J. Halas, and G. Editors, "Shape-Controlled Synthesis and Surface Plasmonic Properties of Metallic Nanostructures," MRS Bull. **30**, 338–348 (2005).
16. S. Kim, J. Jin, Y. J. Kim, I. Y. Park, Y. Kim, and S. W. Kim, "High-harmonic generation by resonant plasmon field enhancement," Nature **453**(7196), 757–760 (2008).
17. A. Taflove, and S. Hagness, Computational Electrodynamics: the Finite-Difference Time-Domain Method, (Arthech House, London, 2000).
18. E. D. Palik, Handbook of optical constants of solids III, (Academic Press, 1998).
19. U. Kreibig, and M. Vollmer, Optical Properties of Metal Clusters (Springer, Berlin, 1995).
20. C. Bohren, and D. Huffman, Absorption and Scattering of Light by Small Particles, (J. Wiley, New York, 1983).
21. M. D. Malinsky, K. L. Kelly, G. C. Schatz, and R. P. V. Duyne, "Chain length dependence and sensing capabilities of the localized surface plasmon resonance of silver nanoparticles chemically modified with alkanethiol self-assembled monolayers," J. Am. Chem. Soc. **123**(7), 1471–1482 (2001).
22. L. J. Sherry, S. H. Chang, G. C. Schatz, R. P. Van Duyne, B. J. Wiley, and Y. Xia, "Localized surface plasmon resonance spectroscopy of single silver nanocubes," Nano Lett. **5**(10), 2034–2038 (2005).
23. V. F. Weisskopf, "Recent development in the theory of the electron," Rev. Mod. Phys. **21**(2), 305–315 (1949).
24. C. L. Haynes, and R. P. V. Duyne, "Nanosphere lithography: a versatile nanofabrication tool for studies of size-dependent nanoparticle optics," J. Phys. Chem. B **105**(24), 5599–5611 (2001).

#113653 - $15.00 USD Received 1 Jul 2009; revised 24 Jul 2009; accepted 25 Jul 2009; published 10 Aug 2009

1. Introduction

Noble metal nanostructures are increasingly enabling practically important applications such as localized surface plasmon resonance (LSPR) [1–3]. In LSPR, a nanostructure absorbs and scatters light, resulting in an extinction spectrum (also called LSPR spectrum) that can be measured by a spectrometer. The LSPR spectrum of a nanostructure depends strongly on its size, shape and composition [4,5], and exhibits high sensitivity to environmental changes. Due to these characteristics, nanostructures have potential utility in immunoassays and other biochemical sensing applications [6–8]. Current research in this area is focusing on the use of various non-spherical nanostructures, such as nanorods, nanocubes, rhombic and triangular nanostructures [9–13], all of which are shapes with sharp vertices and edges.

Rapid development of LSPR sensor research is being promoted by the growing expertise in fabrication methods that allow nanostructures to be realized, such as nanosphere lithography (NSL), electron-beam lithography (EBL), and focused ion-beam (FIB) lithography [14,15]. All nanofabrication techniques have limitations on their ability to reproduce nanostructures as designed, however [15,16]. For example, the resolution of the best-established and the most versatile technique, EBL, is always more than 2 nm, typically 5 nm to 10 nm [15]. Perhaps more importantly for these applications, the sharp features, such as corners and edges, of a certain designed structure are often truncated [16]. The corner features of a nanostructure have great influence on its optical properties and well-defined vertices can markedly improve the quality of the local electromagnetic field.

The work presented herein utilizes a typical two-dimensional array of silver triangular nanoplates to study the impact of truncated vertices on LSPR sensing with polyhedral nanostructures. Numerical models of nanostructures with different truncation ratios are created and the finite difference time domain (FDTD) method is employed to explore the effect of truncated vertices on the electromagnetic field of the nanostructures. Following this analysis, experimental results are generated using an array of triangular nanoplates fabricated with NSL. These results are correlated to the previously generated model to show how truncated vertices of nanostructures predictably degrade their optical properties.

2. Numerical models and electrodynamics results

In this work, the idealized structure is represented as a triangular plate with an equilateral base (consisting of three straight edges and three vertices), which has a height h = 50 nm and an edge length of a = 156 nm, as shown in Fig. 1(a). Following vertex truncation, the nanostructure exhibits truncated vertices [16] as shown in Fig. 1 (b). FDTD calculations have been performed for arrays of triangular plates with truncated vertices arranged in a hexagonal form with a period of 520 nm, the vertex truncation is assumed to be formed by a symmetric circular arc tangent to each of two edges of the triangle. The truncation length, t, defined as the distance between a vertex of the triangle and the closest point of tangency, has a value of 0, 5, 10, 12, 15,

#113653 - $15.00 USD Received 1 Jul 2009; revised 24 Jul 2009; accepted 25 Jul 2009; published 10 Aug 2009

20, or 25 nm. The extent of vertex truncation is characterized by the truncation ratio, which is defined as $\sigma = t/a$.

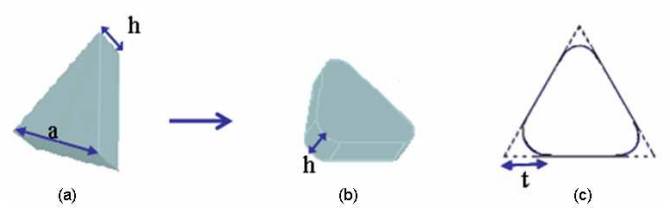

Fig. 1. Triangular nanoplate structures. (a) An idealized triangular nanoplate. (b) A triangular nanoplate with truncated vertices. (c) The vertex truncation is assumed to be formed by a symmetric circular arc tangent to each of the two edges. The truncation length, *t*, is defined as the distance between the vertex of the triangle and the point of tangency.

The transverse magnetic (TM) Maxwell curl equations, shown below in Eqs. (1) – (3), are solved using the FDTD numerical method to generate results [17]:

$$\frac{\partial H_y}{\partial t} = -\frac{1}{\mu_0}\left(\frac{\partial E_x}{\partial z} - \frac{\partial E_z}{\partial x}\right), \tag{1}$$

$$\frac{\partial E_x}{\partial t} = -\frac{1}{\varepsilon}\frac{\partial H_y}{\partial z}, \tag{2}$$

$$\frac{\partial E_z}{\partial t} = -\frac{1}{\varepsilon}\frac{\partial H_y}{\partial x}, \tag{3}$$

where H and E are the magnetic and the electric field, respectively, and their subscript x, y and z denote the three electromagnetic field components. Here, μ_0 is the magnetic permeability in vacuum, $\varepsilon = \varepsilon_0\varepsilon_r$ is the permittivity of the nanostructure material, with ε_0 the permittivity of the vacuum, and ε_r the materials' relative permittivity. For silver in this work, the values of ε_r as a function of wavelength are obtained from Palik [18]. The extinction cross section of the array of nanoparticles is defined as:

$$C_{ext}(\omega) = C_{scat}(\omega) + C_{abs}(\omega) = \frac{P_{scat} + P_{abs}}{I_{inc}(\omega)}, \tag{4}$$

The power transmission parameter P is obtained in terms of the Poynting vector: $\vec{P} = \vec{E} \times \vec{H}$, and the subscripts ext, scat, abs and inc represent extinction, scatter, absorption and incidence, respectively. In our calculations, the substrate is assumed to be glass with an area slightly larger than that of the target nanoplates array and a refractive index of 1.51. The surrounding medium around the nanostructures is assumed to be air with a refractive index of 1.0, and the light source is modeled as non-polarized in order to imitate natural light.

According to the calculated extinction spectra presented in Fig. 2 (a), the localized surface plasmon resonance extinction spectrum exhibits a peak at about 741 nm for the idealized

#113653 - $15.00 USD Received 1 Jul 2009; revised 24 Jul 2009; accepted 25 Jul 2009; published 10 Aug 2009

structure (σ = 0). As indicated in Fig. 2 (b), the peak wavelength of the LSPR spectrum shifts from 741 nm to 650 nm gradually when the truncation ratio σ varies from 0 to 16%. This phenomenon is caused by the retardation effects of the electromagnetic field across the particles as the characteristic size of the nanoparticles decreases [19].

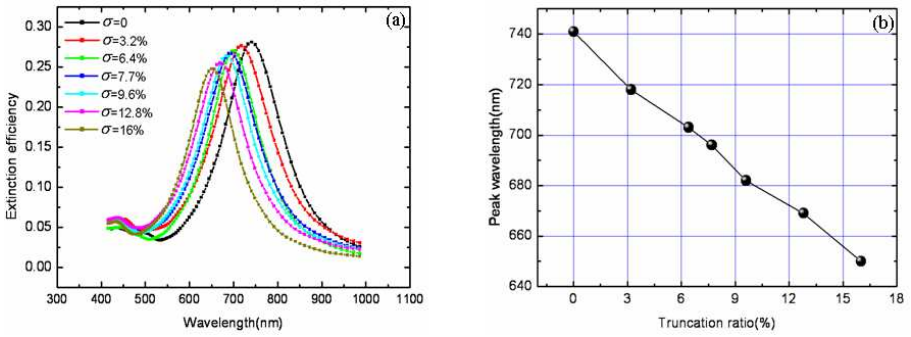

Fig. 2. Calculation results of a triangular nanoplates array with a truncated length t = 0, 5, 10, 12, 15, 20 and 25 nm, with (a) Extinction spectra distributions and (b) peak wavelength distribution extracted from (a)

The extinction efficiency in Fig. 2(a) is based on the surface enhanced mechanism [19,20], which intensifies the local electric field (E-field) at the vertices of the nanostructures. Comparing Fig. 3(a) with Fig. 3(b), it is apparent that the E-field distribution of structures with sharp vertices is more localized than that of the truncated structure with a truncation ratio σ of 12.8%, and the maximal field enhancement of the idealized structure is about 10 times that of the truncated one, as shown in Figs. 3(c) and 3(d). Apparently, it is the less effective concentration of the E-field near the vertices that contributes to the decrease in extinction efficiency of truncated structures (Fig. 2(a)).

#113653 - $15.00 USD Received 1 Jul 2009; revised 24 Jul 2009; accepted 25 Jul 2009; published 10 Aug 2009

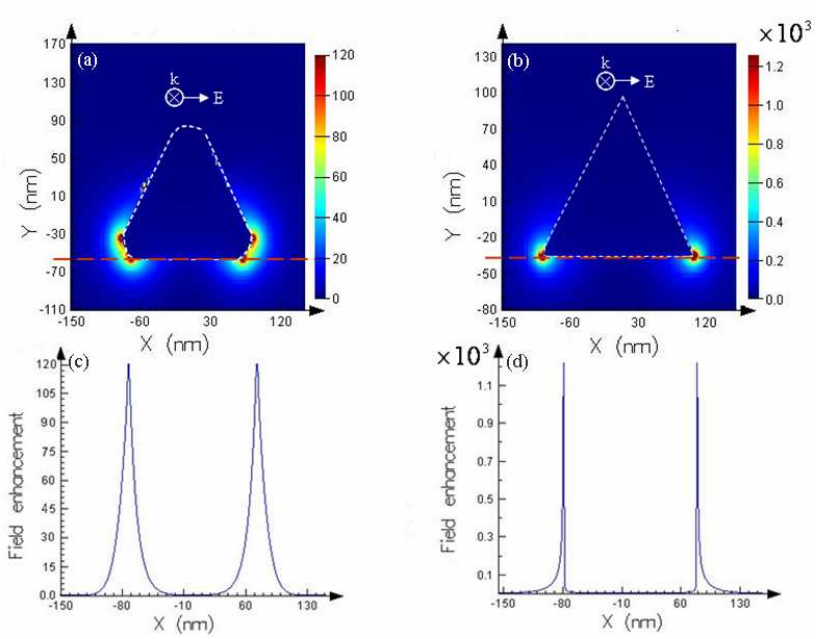

Fig. 3. Field enhancement of local E-fields of nanostructures with a truncation ratio σ of 12.8% (a) and the idealized structure (b). The E-field enhancement profile is presented along the hemline for a truncated structure (c) and the idealized structure (d). The E-fields are excited at their LSPR peak wavelength of 669 nm and 741 nm, respectively.

To further investigate the influence of truncated vertices on the sensitivity of the optical nanostructures, we have also performed the FDTD calculations to explore the refractive index sensitivity of the nanostructures with different truncation ratios. The refractive index sensitivity for a LSPR sensor is defined as: $m = \Delta\lambda_p / \Delta n$, where $\Delta\lambda_p$ and Δn denotes peak wavelength shift in a different medium and the corresponding refractive index change [21]. For an idealized structure, the peak wavelength shifts higher when the refractive index increases, and the refractive index sensitivity m is as large as 434 nm/RIU (refractive index unit) (Fig. 4(a)). The refractive index sensitivity decreases strongly when σ increases from 0 to 3.2%, as shown in Fig. 4 (b). This indicates that nanoparticles with sharp vertices exhibit high sensitivity while the performance of nanoparticles with slightly rounded vertices is much poorer. When σ varies from 6.4% to 16%, the refractive indices fall from 336 nm/RIU to 250 nm/RIU. It should be noted that the refractive index sensitivity shown in Fig. 4(b) has an almost identical relationship to truncation ratio as the extinction spectra peak wavelength as shown in Fig. 2(b). This can be explained using quasistatic theory: if the real part of the dielectric function ε_1 is approximated as varying linearly with wavelength, the refractive index sensitivity m is approximately linear with the extinction spectra peak wavelength [5].

#113653 - $15.00 USD Received 1 Jul 2009; revised 24 Jul 2009; accepted 25 Jul 2009; published 10 Aug 2009

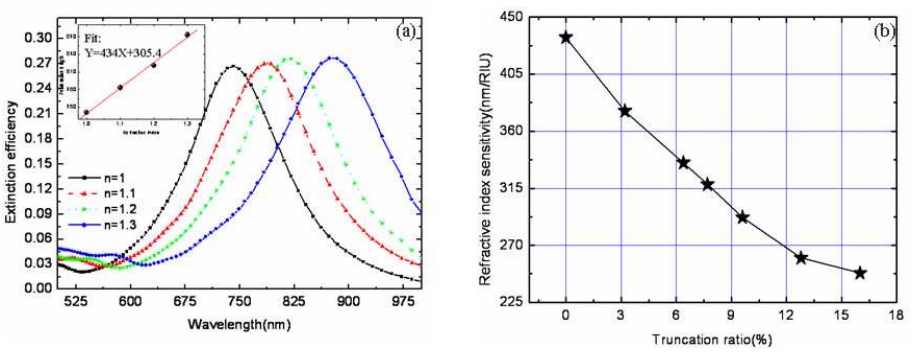

Fig. 4. (a) Extinction spectra of an idealized structure in different media and the obtained refractive index curve and (b) Refractive index sensitivity distribution of truncated structures with truncation ratio σ = 0, 3.2%, 6.4%, 7.7%, 9.6%, 12.8%, or 16%.

The overall LSPR sensing performance of a nanostructure is evaluated by the figure of merit (FOM), which is defined as [22]:

$$\text{FOM} = m / \text{FWHM}, \tag{5}$$

where FWHM is the full-width at half-maximum of the LSPR spectrum in air (n = 0). Unlike the refractive index sensitivity, which is an extrinsic parameter, FWHM is intrinsically determined by the shape of a nanostructure and is used to evaluate the resolution factor. The calculated FOM values decline as the truncation ratio increases, as shown by the fitted curve in Fig. 5. According to this relationship, when $\sigma \geq 10\%$, the FOM is lower than 2.0%, and this results in much poorer sensing performance by the nanostructures array. The small variations of FOM values (hollow circles in Fig. 5) are probably caused by the random energy level splitting of free electrons in metals [23].

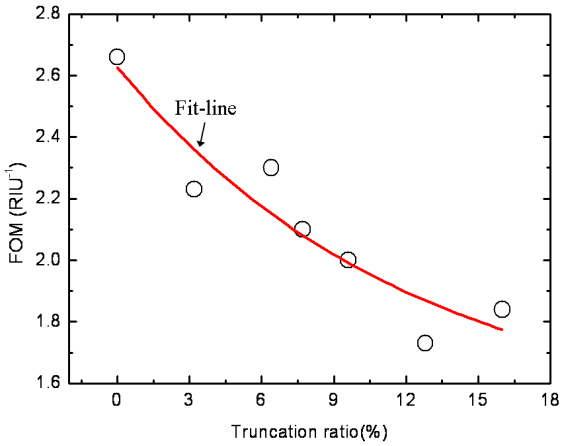

Fig. 5. Figure of merit distributions for different truncation ratios

#113653 - $15.00 USD Received 1 Jul 2009; revised 24 Jul 2009; accepted 25 Jul 2009; published 10 Aug 2009

3. Experiment results and analysis

The designed nanostructures with idealized corner features were arrayed in a hexagonal form with a period of 520 nm (Fig. 6 (a)) and were fabricated by the NSL fabrication method. NSL is one of the most popular means to fabricate nanoscale structures due to its cost-effectiveness and its speed in producing periodic arrays of a large area with a specific particle shape, placement, and orientation [15,24]. This also makes it an ideal method for studying the effect of truncated vertices on the optical properties of nanostructures. The fabrication process primarily consists of three steps: first, a polystyrene (PS) nanospheres colloidal suspension was dispensed onto the K9 glass substrate with a refractive index of 1.51, which is coincident with simulation assumption in Section 2, and a large-area close-packed nanosphere monolayer was patterned by changing the solution concentration, drying conditions, and surface properties; second, a layer of silver was deposited on the monolayer template in a thermal evaporator (400-I, C-Vac inc. China); and third, the PS nanospheres were removed using ethanol in an ultrasonic bath. The designed nanostructures then appeared on the glass chip, as shown in the scanning electron microscopy (SEM) image (Fig. 6 (b)). The sharp features were inevitably damaged by the physical evaporation in step 2 and the chemical modification in step 3, changing the idealized structures into truncated ones as discussed earlier. The truncation ratio of the fabricated nanostructures was found to be approximately 12.8% by examining an enlarged image of one of the fabricated nanostructures as shown in Fig. 6(b).

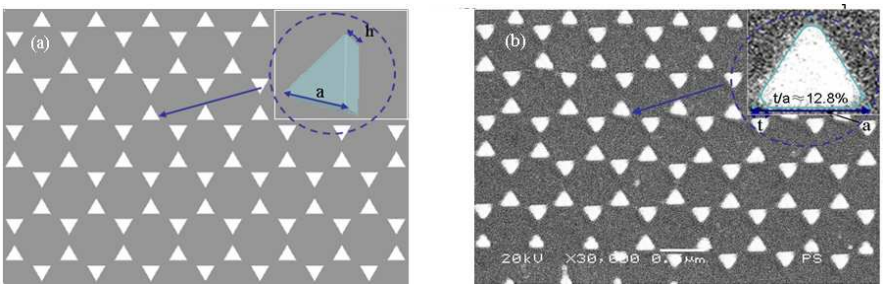

Fig. 6. (a) the designed nanostructures with sharp vertices and (b) SEM image of the corresponding fabricated nanostructures.

The LSPR-based extinction spectra of the fabricated Ag nanostructures were measured both in clean air (n≈1.0) and absolute alcohol (n≈1.37) at room temperature (20°C) by an UV-vis-NIR spectrometer (QE65000, Ocean Optics inc. America), with associated data processing software. For n = 1.0, the peak wavelength was measured to be approximately 670 nm (Fig. 7(a)), which closely matches the calculated result for a truncated structure with a truncation ratio σ of 12.8%. This result differs by approximately 71 nm with that of the idealized structure as shown in Fig. 7(a). The measured extinction spectrum shows good agreement for n = 1.37, with results similar to those calculated for $\sigma = 12.8\%$. Both the SEM image and the measured extinction spectra confirm that the fabricated nanostructure has an

#113653 - $15.00 USD Received 1 Jul 2009; revised 24 Jul 2009; accepted 25 Jul 2009; published 10 Aug 2009

average truncation ratio approximately of 12.8%, and that truncated vertices strongly influence the optical properties of nanostructures for a LSPR sensor.

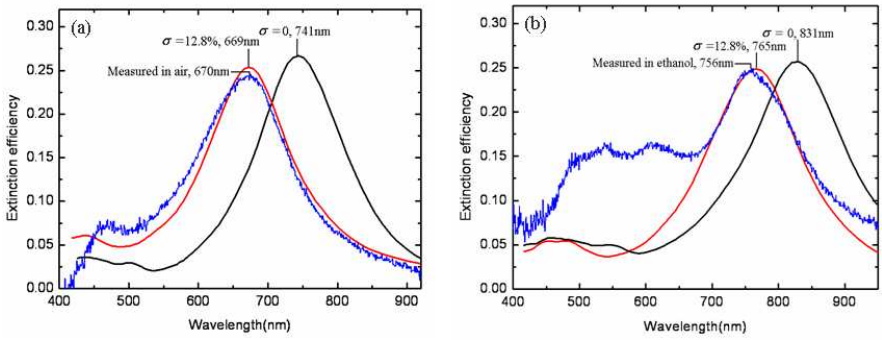

Fig. 7. Extinction spectra obtained from simulations and experiments: (a) in air, and (b) in ethanol.

The refractive index sensitivity for the fabricated structure can be calculated as $m = (756\text{ nm} - 670\text{ nm})/(0.37\text{ RIU}) \approx 232.4$ nm/RIU , and the FWHM of the LSPR spectrum in air is about 160 nm (see Fig. 7(a)). Therefore, FOM ≈1.45 RIU^{-1}as calculated. This is much smaller than that of the idealized structure, 2.66RIU^{-1}, indicating that the performance of the fabricated LSPR sensor with truncated corners is greatly reduced. It should be noted that the test FOM of 1.45 RIU^{-1}has a small difference with that of the simulation result for $\sigma = 12.8\%$ of 1.73 RIU^{-1}. This can be attributed to two factors. First, the characteristic sizes and the shapes of fabricated nanostructures array are not as homogeneous as considered in the simulation. As a result, the FWHM of the extinction spectrum in air for the fabricated nanostructures is a little wider than the simulation results. Second, the impurities in the medium and manipulation errors significantly influence the test extinction spectra, especially the spectra in ethanol medium, which further influence the test refractive index sensitivity. The sensing performance of the fabricated nanostructures will be further improved when the sample is measured in N_2 medium without dust and vapor.

4. Conclusion

This work presents a study on the effects of truncated vertices on the optical properties of polyhedral nanostructures by combined simulations and experiments. Both the electrodynamics analysis and the experimental results demonstrate the great influence of truncated vertices on the performance of a LSPR sensor. Simulation results indicate that the peak wavelength of a LSPR spectrum shifts blue and the FOM of sensing performance becomes poorer when the truncation ratio increases, as a result of the depressed E-field at the truncated vertices. The corresponding fabricated triangular nanoplate array was shown to have

#113653 - $15.00 USD Received 1 Jul 2009; revised 24 Jul 2009; accepted 25 Jul 2009; published 10 Aug 2009

a truncation ratio of 12.8%, which is consistent with the simulation results. This study is expected to provide guidlines for both designing and fabricating a nanostructure for LSPR sensing.

Acknowledgements

This work was supported by the Natural Science Foundation of China (60736037) and the Opening Project of Key Laboratory of Low Dimensional Quantum Structures and Quantum Control (Hunan Normal University), Ministry of Education, (QSQC0909).

#113653 - $15.00 USD Received 1 Jul 2009; revised 24 Jul 2009; accepted 25 Jul 2009; published 10 Aug 2009